Bulletin of the Seismological Society of America, Vol. 97, No. 2, pp. 614–623, April 2007, doi: 10.1785/0120060111

Determination of Shallow Shear-Wave Velocity at Mississippi Embayment Sites Using Vertical Seismic Profiling Data

by Jiandang Ge, Jose Pujol, Shahram Pezeshk, and Scott Stovall

Abstract We used vertical seismic profiling (VSP) data collected in shallow boreholes (about 40–60 m deep) to determine the shear-wave velocity at four sites in the Mississippi embayment in southwestern Tennessee. The source was an air-powered hammer that produces repeatable *SH* waves, which were recorded by source monitor geophones deployed on the surface very close to the source. Three approaches were used to determine interval velocities: an approximate zero-offset method, a layer-stripping method, and a waveform-matching method. The first two methods use arrival-time picks, whereas the latter is based on the fit of synthetic VSP data to the first half-cycle (approximately) of each trace. The advantage of this method over the other two is that it uses a segment of the data, rather than a single data point. Therefore, the velocities determined using the waveform-matching method are better constrained and are not affected by picking errors, which may translate into significant spurious velocity variations. The source wavelets recorded by one of the monitor geophones and the velocity model computed with the layer-stripping method were used to generate synthetic vertical seismic profiling data for comparison with the actual data. Then the model velocities were modified interactively, one layer at a time, until a satisfactory match was achieved. This required including attenuation in the computation of the synthetic data. The four sites investigated in this study can be divided into two groups: low-velocity sites (Shelby Farms and Covington) and high-velocity sites (Brownsville and Jackson). These last two sites are at larger distances from the embayment axis than the other two, which means that the difference in velocities probably corresponds to the presence of different geologic units. Good agreements between the lithology in the boreholes and the velocity profiles were obtained for all the four sites.

Introduction

The upper Mississippi embayment is a large south-southwest-plunging structural syncline (Stearns and Marcher, 1962) filled with low-velocity, poorly consolidated Cretaceous and Cenozoic sediments that overlie high-velocity Paleozoic rocks. The sedimentary record indicates that the most recent subsidence occurred in the late Cretaceous through Eocene times (Stearns and Marcher, 1962), possibly as the result of crustal thinning and thermal contraction (Kane *et al.*, 1981). The thickness of the post-Paleozoic sediments reaches about 1 km in the Memphis area (Fig. 1).

Because of the potential for a large earthquake in the New Madrid seismic zone (NMSZ) and the increase in the seismic hazard introduced by the presence of the embayment sediments, there is considerable interest in determining their shear-wave velocities, which are a good indicator of the ground motions that can be expected in case of an earthquake (e.g., Field *et al.*, 2000, and references therein). Chen *et al.* (1996) used *S*-to-*P* converted waves to determine the *S*-wave velocities of sediments in the central part of the NMSZ and found that they vary between 0.45 km/sec and 0.67 km/sec, with the larger values corresponding to areas where the sediments are thicker. These velocities are much lower than the *S*-wave velocity of the Paleozoic rocks (about 3.4 km/sec) and this high-velocity contrast may lead to a large amplification of the ground motion in case of an earthquake (e.g., Pujol *et al.*, 2002). However, the National Earthquake Hazards Reduction Program (NEHRP) recommended provisions for buildings, and other constructions require the use of the average shear-wave velocities in the upper 30 m (Federal Emergency Management Agency [FEMA], 1997). Street *et al.* (2001) determined the shallow-wave velocities at nearly 400 sites in the upper Mississippi embayment by using reflection and refraction techniques. In addition, there is also a good amount of velocity information available for the greater Memphis area, summarized by Romero and Rix (2001). These velocities were determined by using mostly

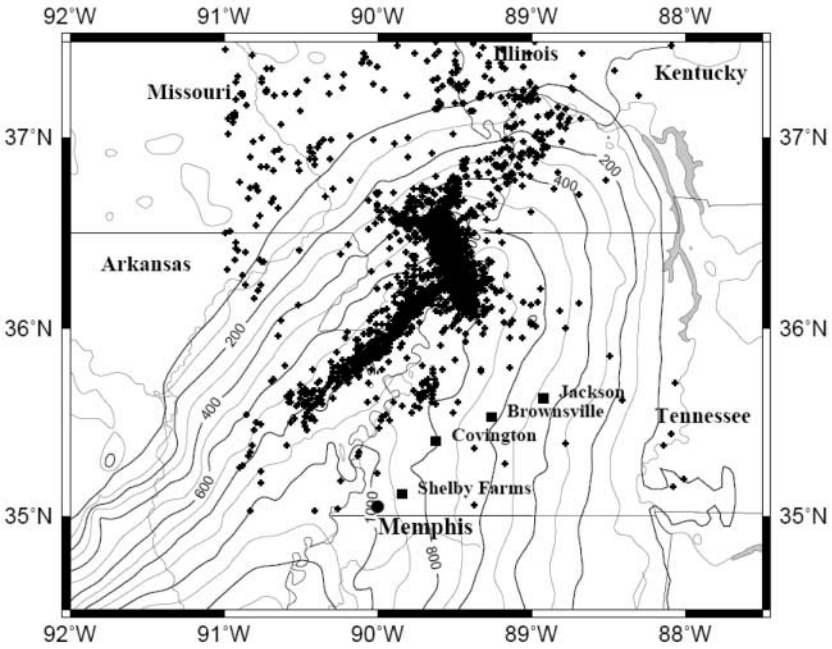

Figure 1. Map of the upper Mississippi embayment. The contour lines indicate the thickness of the unconsolidated sediments. Filled squares show the locations of VSP data collection. Crosses indicate the epicenters of microearthquakes within the NMSZ.

refraction techniques, although seismic core penetration test (SCPT) data as well as data collected in one borehole have been used. In this article we describe the determination of shallow shear-wave velocities by using seismic data recorded in boreholes drilled between 17 and 118 km away from Memphis. The method used for velocity determination is based on waveform matching, which reduces the errors in the computed velocities. As shown here, the velocities computed using arrival-time picks may be affected by considerable errors when the data are affected by noise. The velocities we determined show a spatial pattern, with higher values away from the axis of the embayment.

Data

The vertical seismic profiling (VSP) data used in this research were collected in four boreholes drilled in western Tennessee (Fig. 1) and cased with 3-inch PVC pipe. The borehole depths ranged between 40 and 60 m. An air-powered impulsive shear-wave source similar to that used by Liu *et al.* (1996) was used in the experiments. The source has a hammer that moves in both directions along low-friction tracks and hits two anvils located on both sides of the hammer. The triggering system is based on a glass reed switch. The traces corresponding to the two hammer directions have opposite polarities. A van resting on the shear-wave source gives a good coupling to the ground. The downhole receiver consists of two three-component velocity sensors with natural frequencies of 4.5 and 10 Hz encased in a water-proof PVC pipe. The clamping mechanism consists of a steel spring compressed by a DC electric motor. To monitor the quality of the data, 4.5 Hz and 10 Hz three-component surface geophones were placed close to the source. A 16-channel 16-bit analog-to-digital data acquisition card was used to record the data. In all cases the geophone spacing was 1.5 m (5 ft) and the source offset (i.e., the distance to the borehole) was 1.2 m (4 ft). For each depth, four hits were recorded, two in each direction. As the recording depth increased, a higher amplification was applied to the downhole geophones to account for the effects of geometric spreading and attenuation. The sampling interval was 0.67 msec.

Methods

Three methods were used to determine the velocity structure: (a) an approximate method that assumes zero source offset, (b) a layer-stripping method that takes into account the offset, and (c) a waveform-matching method based on the comparison of actual waveforms and synthetic waveforms generated by using software that assumes normal incidence. The first method was used to see how much error in the computed velocities is introduced by the zero-offset approximation.

Approximate Zero-Offset Method

The interval velocity between two depths Z_a and Z_b ($>Z_a$) is given by

$$V = \frac{Z_b - Z_a}{T_b - T_a}, \tag{1}$$

where T_a and T_b are the wave-arrival times at depths Z_a and Z_b, respectively. Usually, Z_a and Z_b are adjacent depths in the survey. Interval velocities will be referred to as layer velocities, although Z_a and Z_b do not necessarily constitute actual layer boundaries.

Layer-Stripping Method

This method takes into account the source offset and is based on the computation of the velocities one layer at a time, starting with the shallowest one (Pujol *et al.*, 1985). To explain the method, let us consider a two-layer model (Fig. 2). The thickness and velocity for the upper layer are H_1 and V_1, respectively, and are H_2 and V_2 for the second layer. The source offset is D. The arrival times at the first and second geophones are T_1 and T_2, respectively. Based on the geometry of Figure 2, the velocity in the upper layer is:

$$V_1 = \frac{\sqrt{D^2 + H_1^2}}{T_1}. \tag{2}$$

Now consider a ray arriving at the second geophone. For this ray the travel time in the first layer is:

$$\Delta t_1 = \frac{H_1}{V_1 \cdot \cos \beta} \tag{3}$$

where β is the take-off angle. Therefore, the travel time in the second layer is $T_2 - \Delta t_1$ and the velocity in the second layer can be computed from

$$V_2 = \frac{\sqrt{(D - H_1 \cdot \tan \beta)^2 + H_2^2}}{T_2 - \Delta t_1} \tag{4}$$

Alternatively, the velocity can be computed using Snell's law

$$V_2' = \frac{V_1 \cdot (D - H_1 \cdot \tan \beta)}{\sin \beta \cdot \sqrt{(D - H_1 \cdot \tan \beta)^2 + H_2^2}} \tag{5}$$

Note that there is no arrival-time information in equation (5). For arbitrary β these two velocities will be different, and to make them equal we change the take-off angle iteratively until the difference between the two velocities is sufficiently small. Once the velocity for the second layer has been computed, a similar process allows computation of the velocities for the other layers.

Waveform-Matching Method

The velocities determined using the previous two methods may be affected by errors associated with manually picking the first arrivals. To illustrate the errors that can be introduced, consider the following example. The vertical travel time in a layer 1.5 m thick with a velocity of 300 m/sec is 5 msec. If the error in arrival times is within ± 1 msec, the velocities computed for the layer will be between 250 m/sec and 375 m/sec. The analysis of the actual data below indicates that this kind of error may affect the velocities computed using the other two methods. The waveform-matching method provides a convenient way to reduce them because it uses a larger portion of the recorded information. A similar approach was used by Stewart (1983).

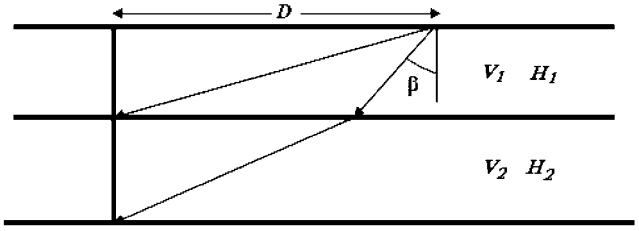

Figure 2. Geometry for the determination of interval velocities using the layer-stripping method. The horizontal and vertical bold lines represent layer boundaries and a borehole, respectively. The subscripted V and H and D indicate layer velocity and thickness and source offset, respectively.

To generate the synthetic VSP data we used software developed by Wu (1983), and because the only reference to this software is a thesis, its lineage and basic features are sketched here. Wuenschel (1960) described the generation of synthetic seismograms for vertical incidence and perfectly elastic layered media using the matrix theory approach of Thomson (1950). Sherwood and Trorey (1965) extended the Wuenschel formulation to include anelastic attenuation. Their method was based on a z-transform approach, which limited their models to layers of equal travel time. Butler (1979) removed this limitation by working in the frequency domain while preserving the matrix formulation. Finally, Wu (1983) modified Butler's approach to make it computationally more efficient and to include dispersion as an option. The earth model consists of a sequence of horizontal layers between two half-spaces. The elastic parameters and attenuation are constant in each layer. The layer thicknesses are arbitrary and the synthetic seismograms are computed at each layer boundary. Because of the assumption of vertical incidence, wave propagation is represented by the one-dimensional wave equation, namely,

$$v^2 \frac{\partial^2 u(x,t)}{\partial^2 x} = \frac{\partial^2 u(x,t)}{\partial^2 t} \tag{6}$$

which applies to *P* and *SH* waves. Moreover, the reflection and transmission coefficients for normal incidence have similar expressions for the two types of waves (see problems 4.11–12 and 6.10 and equations 6.6.50–51 of Pujol [2003]). In terms of harmonic waves, attenuation is represented by the standard exponential decay, namely,

$$u(x,t) = u_0 e^{-\omega x/2Qc} e^{i(\omega t - kx)} \tag{7}$$

where u_0 is a constant, Q is the quality factor, c is the phase velocity, and ω and k are angular frequency and wave number, respectively. A convenient way to introduce attenuation

is to let the velocity in equation (6) be complex. Wu (1983) used the following expression for v

$$v = \frac{c}{1 - i/2Q} \tag{8}$$

(see equations 11.8.12–13 of Pujol [2003]). Dispersion was introduced using

$$c(\omega) = c_0\left(1 + \frac{1}{\pi Q_0} \ln \frac{\omega}{\omega_0}\right), \tag{9}$$

where ω_0 indicates a reference frequency, $c_0 = c(\omega_0)$, and $Q_0 = Q(\omega_0)$. Equation (9) follows from an equation derived by Futterman (1962) (see §11.7 of Pujol, 2003). In Futterman's work, Q is a slowly varying function of ω and for practical purposes it can be taken as constant over relatively wide frequency ranges. The output of the program is the impulse response in the frequency domain computed at equispaced values. The transformation to the time domain is done using the fast Fourier transform (Wilson, 1990), which requires arranging the data as described in, for example, Brigham (1974). The resulting time-domain impulse response is finally convolved with the desired source time function. An example of the synthetic data produced by this software is shown in Figure 3. The corresponding earth model is given in Table 1. Because the value of Q (equal to 1000) is large, the data do not show attenuation. The high-frequency noise seen in the impulse response is due to the choice of the number of frequencies used in the computations and the frequency spacing. This noise, however, is not important because it is filtered out by the source time func-

Table 1
Velocity Model Used to Generate a Synthetic VSP

Velocity (m/sec)	Layer Thickness (m)
250	15.0
250	1.5
300	1.5
300	1.5
400	1.5
400	1.5
500	1.5
500	1.5
200	1.5
200	1.5
500	1.5
500	1.5
600	1.5
600	1.5
700	1.5
400	1.5
400	1.5

$Q = 1000$. Density = 2.0 g/cc.

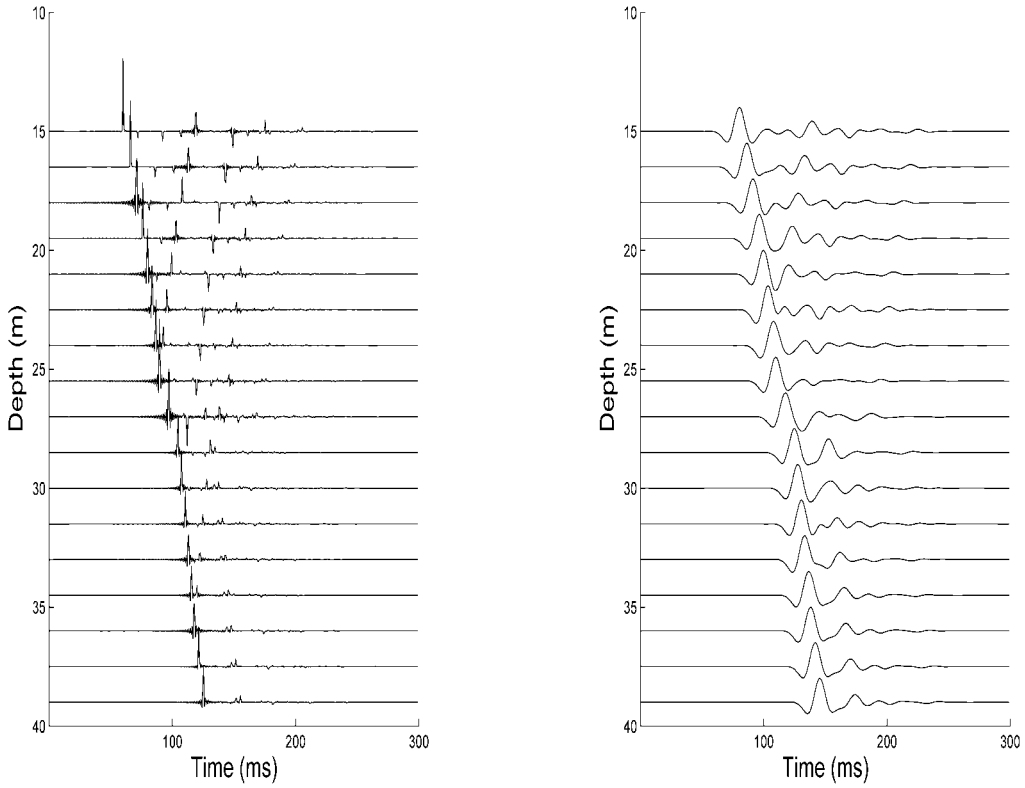

Figure 3. (Left) Impulse response for the model in Table 1. (Right) Corresponding synthetic VSP generated by convolution with a Ricker wavelet. Each trace has been normalized with respect to its largest amplitude.

tion, which is a Ricker wavelet with a peak frequency of 39 Hz. This value is typical of the peak frequencies that characterize the actual VSP data. Note the strong reflections caused by several abrupt changes in velocity.

The generation of synthetic data for comparison with the actual data is done as follows. The first cycles of the traces recorded by the monitor geophones are used as source time functions, whereas the initial velocity model is that determined with the layer-stripping method. Then this model is modified iteratively until the synthetic data match (i.e., overlap) the actual data in the vicinity of the first arrivals (approximately the first half-cycle). However, for a good match between synthetic and actual data it is necessary to account for attenuation correctly, which is done using results obtained by Ge (2005), who used the spectral ratio method to compute attenuation. A detailed description of the method can be found in Pujol *et al.* (2002). The procedure of accounting for attenuation in the waveform-modeling method is explained in detail subsequently. The assumption of vertical incidence, required by the software, is justified by the small offsets used, which result in rather small errors in the computed velocities, limited to the upper layers. Representative errors are given in the next section.

Applications

We determined velocities using VSP data recorded in four sites shown in Figure 1. One of the sites is within the Shelby Farms, which is a park approximately 17 km east of Memphis. Figure 4 shows two of the VSPs with different polarities. Because the waves do not have sharp onsets and the data are affected by some noise, the arrival times are determined from the intersection of the two traces for each depth (Fig. 4). Some of the traces had poor quality and were discarded. The velocities determined using the zero-offset and layer stripping methods are shown in Figure 5. Because the offset is small (1.2 m), the two sets of velocities have some differences only for the shallowest depths. For example, the differences are 11% for the 0- to 2.4-m interval and 3% for the 5.5- to 7.0-m interval. Below 11.5 m the two sets are almost indistinguishable. Therefore, we neglected the source offset effect when using the waveform-matching method and assumed zero source offset.

To apply the waveform-matching method we generated synthetic VSP data using the velocity model determined by layer stripping and used the first cycles of the monitor traces as source wavelets. A quality factor equal to 1000 was used. Figure 6 shows that the actual and synthetic data do not match well. For this reason the layer velocities were interactively modified to match (i.e., overlap) the first half-cycles (Fig. 7). The comparison between the actual and synthetic data is visual, and to investigate the error that this approach may introduce in the computed velocities we changed the input velocity for one layer and found that the actual and synthetic waveforms no longer overlap when the velocity variations reach about $\pm 10\%$. Therefore the waveform-matching velocities for this site may be affected by errors on the order of $\pm 10\%$.

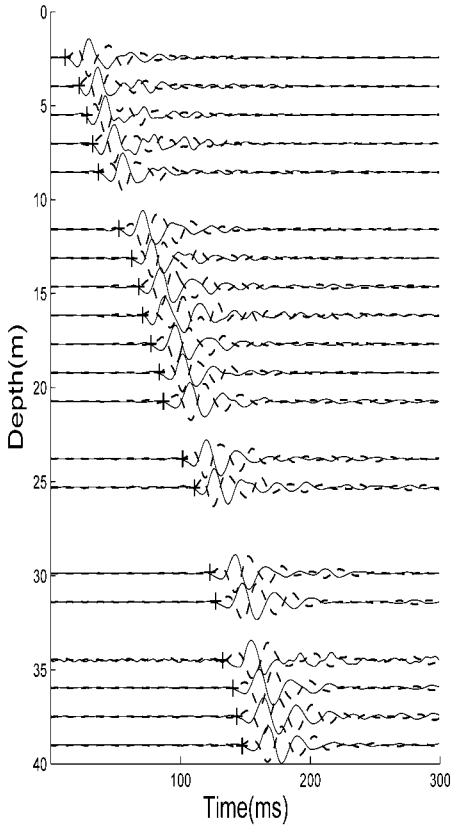

Figure 4. Plot of the Shelby Farms VSP traces for two hammer hits in opposite directions. Crosses indicate arrival-time picks. Some bad traces have been removed.

Although Figure 7 shows a reasonable waveform match, a major obvious difference between the synthetic and actual data is the presence of strong reflections in the former that are not observed in the latter. The reason for this difference is the large value of Q used to generate the synthetics, which means that essentially there is no attenuation. When a realistic value of Q (25.3) is used, the reflections are highly attenuated, which improves the agreement with the actual data (Fig. 7). As noted earlier, the values of Q used for this and the other VSPs were determined by Ge (2005) using a spectral ratio method.

A comparison of the velocity models determined using the three methods (Fig. 5) shows that the velocities from waveform matching have significantly smaller variations as a function of depth than the other two velocities. However, the waveform-matching velocities still have some large variations, and for this reason we will compare them with the lithology described in the borehole-drilling report (Fig. 5). Soil samples were taken during drilling using a split-spoon sampler. Afterward, geotechnical engineering tests were carried out for soil classification purposes. The lithology for this site is characterized by a sequence of sand and clay

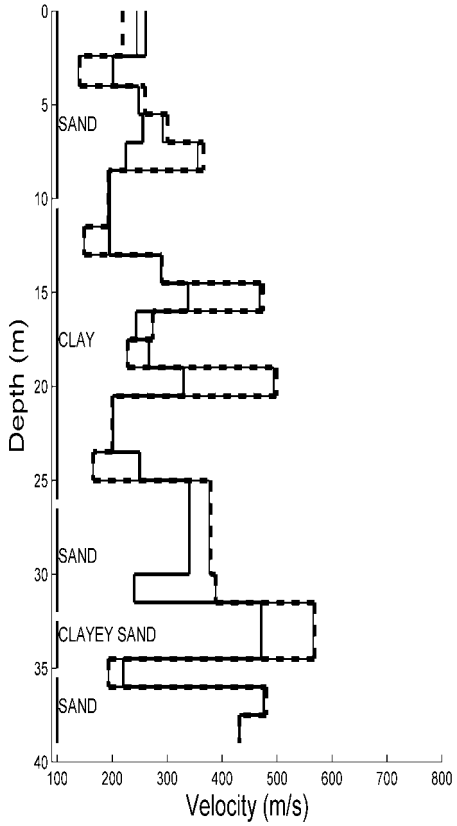

Figure 5. Shelby Farms velocity models obtained using the three methods described in the text. Dashed line, zero-offset method; thin solid line, layer-stripping method; bold line, waveform-matching method. Lithology information is also included. The geographic coordinates (longitude, latitude) for this site are ($-89.84°$, $35.12°$).

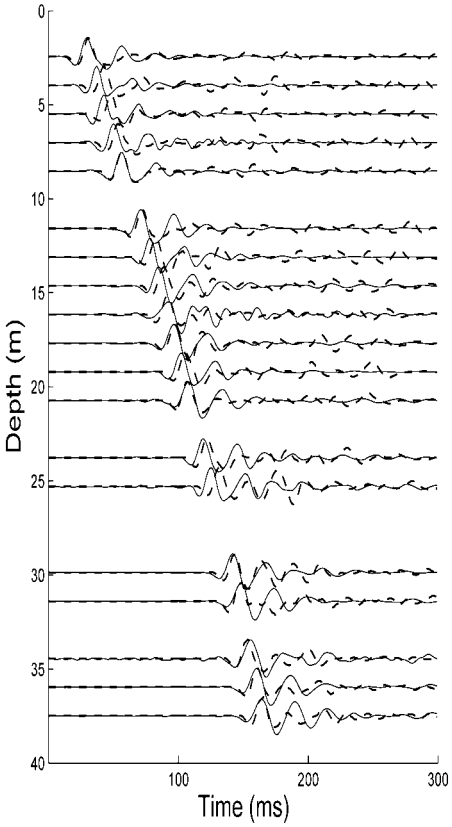

Figure 6. Shelby Farms actual VSP (solid traces) and synthetic VSP (dashed traces) generated by using the first cycles of the corresponding source wavelets and the velocity model determined using the layer-stripping method and a Q-value equal to 1000.

layers, with the main boundaries at about 10 m, 26 m, 32 m, and 35 m, corresponding to sharp velocity variations. It appears, however, that the lithologic profile does not have sufficient detail. For example, from 10 to 26 m the lithology log indicates the presence of a single clay layer, but as the velocity model shows, there should be some lithological variations within this layer.

The data from the other three sites were processed as the Shelby Farms data, with the following results. The actual and synthetic VSP data and velocities are shown in Figures 8, 9, and 10, for the Covington, Jackson, and Brownsville sites, respectively. For the first two sites the differences between the velocity models determined from arrival-time picks and waveform modeling are not as significant as for the Shelby Farms site, probably because the data used allow for more accurate time picks. In contrast, the Brownsville data show significant differences, which should not be surprising given the noise affecting the data. Changing the velocity of one of the layers, as described earlier, shows that the waveform-matching velocities for this site may be affected by errors on the order of $\pm 17\%$.

Discussion

Comparison of the waveform-matching velocities for the four sites investigated here shows that they are higher in Brownsville and Jackson than in Shelby Farms and Covington. Unfortunately, the lithological information available is not sufficient to establish a precise correlation between lithology and velocities. Therefore, the following considerations are rather general (based on Miller *et al.*, 1966). Shelby Farms is on the Quaternary alluvium of the Wolfe river floodplain, the Covington and Brownsville sites are on loess (Quaternary massive clayey and sandy silt), and the Jackson site is on Tertiary sediments. The first three sites are underlain by Tertiary sediments, which are subdivided into three groups: the Claiborne, Wilcox, and Midway groups (e.g., Van Arsdale and TenBrink, 2000), with the first two having a combined thickness of at least 120 m. The Shelby Farms and Covington boreholes are within the Claiborne group, but the Jackson borehole may have encountered the Wilcox group (T. Hart, personal comm., 2006). We do not have reliable information for the Brownsville borehole. We know, however, that the thickness of the Mississippi embayment post-Paleozoic sediments increases toward the axis of the

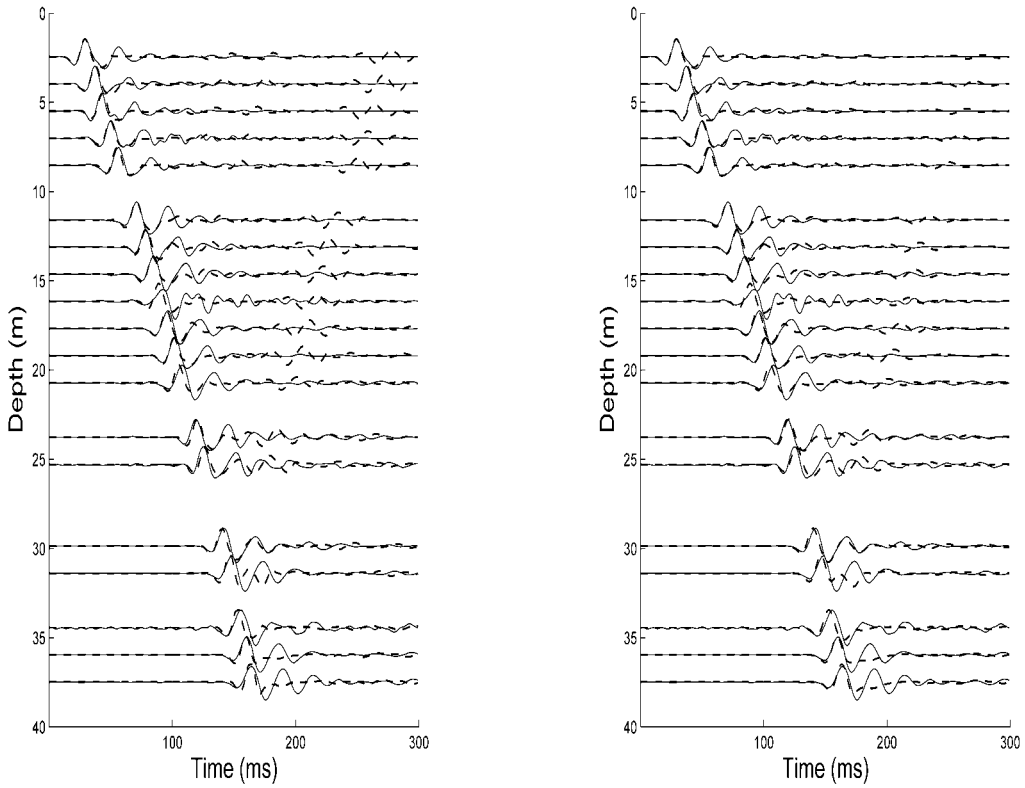

Figure 7. Similar to Figure 6 with the velocities adjusted so that the synthetic VSP traces match the actual ones in the vicinity of the first arrivals. Two values of Q were used, 1000 (left) and 25.3 (right), the latter determined by using a spectral ratio method (Ge, 2005).

embayment (Fig. 1). This also applies to the Tertiary sediments (Van Arsdale and TenBrink, 2000). For example, the top of the Midway group east of Memphis has a thickness difference of 300 to 400 m over a distance of 50 km, which means that for a given depth, the age of the sediments increases to the east. Therefore, the velocity variations that we observed may be due to differences in lithology, sediment age, and sediment consolidation.

The NEHRP provisions require the average shear-wave velocities for the upper 30 meters ($\bar{v}_s$), computed using the following equation (FEMA, 1997):

$$\bar{v}_s = \frac{\sum_{i=1}^{n} d_i}{\sum_{i=1}^{n} d_i / v_{si}}, \tag{10}$$

where d_i and v_{si} indicate layer thickness and velocity, respectively, and the sum of the d_is equals 30 m. For the Shelby Farms, Covington, and Jackson sites the corresponding values are 249, 259, and 330 m/sec, respectively, so that they are classified as class D soils ($180 \leq \bar{v}_s < 360$ m/sec; FEMA, 1997). For Brownsville, $\bar{v}_s$ is 366 m/sec, which would indicate a class C soil ($360 \leq \bar{v}_s < 760$ m/sec; FEMA, 1997). However, because $\bar{v}_s$ is very close to the velocity that defines the boundary between soils C and D, and because the quality of the VSP data was not as good as for the other VSPs, we cannot rule out that the Brownsville soils are of class D.

Although velocities determined using borehole data are better constrained than those determined using data collected on the surface, a clear disadvantage is the need to have boreholes available. For economical reasons, this limits the number of sites that can be investigated, and for this reason it is helpful to compare the velocities computed using the two types of data. A direct comparison is possible for two of our sites because they are close to several sites with $\bar{v}_s$ determined by Street *et al.* (2001) using seismic *SH*-wave reflection and refraction techniques. Their two sites closest to the Jackson borehole are 3 and 12 km away and have velocities of 279 and 332 m/sec, respectively, which are close to our value of 330 m/sec. The two sites closest to the Brownsville borehole are about 8 km away and their velocities are 361 and 410 m/sec, which are close to the 366 m/sec that we determined. These results seem to confirm that the soils at the VSP site are of class C.

Shear-wave velocity information for Shelby Farms has been compiled by Romero and Rix (2001), who used information from seven surveys. Six of them involved SCPT data (e.g., Schneider *et al.*, 2001) and one from a refraction sur-

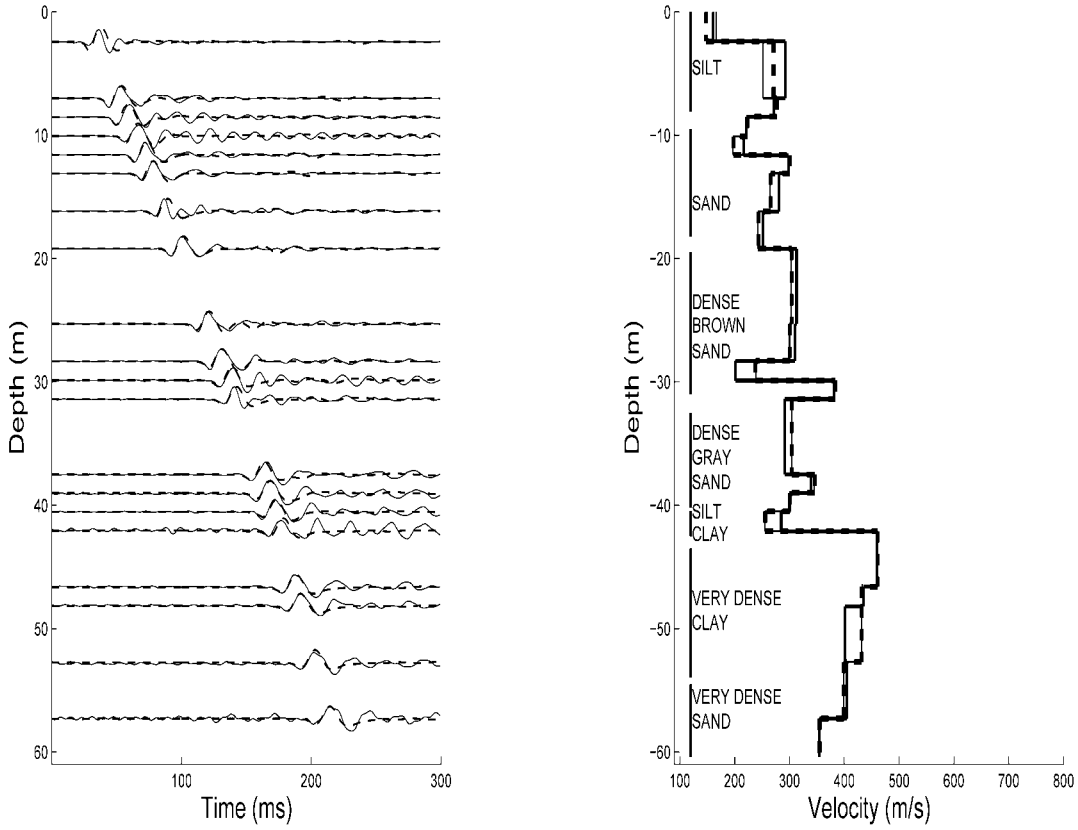

Figure 8. (Left) Covington actual VSP (solid traces) and synthetic VSP (dashed traces) generated for a Q-value of 18.6. (Right) Velocities as in Figure 5. The geographic coordinates (longitude, latitude) for this site are ($-89.63°$, 35.40°).

vey. The average velocity for the upper 21 m is 278 m/sec with a standard deviation of 62 m/sec. For two of the SCPTs the average velocities for the upper 30 m are 239 and 252 m/sec, which are close to the 249 m/sec we determined. The SCPTs are similar to the VSP surveys in that they allow *in situ* measurement of arrival times, but have the advantage that they are less expensive because it is unnecessary to drill boreholes. It must be kept in mind, however, that the SCPT interval velocities may also be affected by errors in arrival-time pickings as well as in the determination of distances (Thitimakorn *et al.*, 2006). Therefore, our conclusions regarding the VSP velocities derived using conventional methods also apply to the SCPT velocities.

Conclusions

Shallow shear-wave velocity models were determined for four sites in western Tennessee using borehole data. To ensure that the computed velocities were not affected by errors in arrival-time picks, which can be significant, we used a method based on the matching of synthetic VSP data to the first half-cycle (approximately) of each trace. Because the velocities determined by waveform matching are constrained by a segment of each trace, they are less affected by errors than those determined using the conventional methods, which rely on just one point per trace. The computed velocities are higher for the Brownsville and Jackson sites, which are to the east of the other two, Shelby Farms and Covington. This variation is probably related to sediment age, lithology, and consolidation, but the geological information available precludes establishing a more precise correlation. The average velocities for the Shelby Farms, Covington, and Jackson sites in the upper 30 m range between 249 and 330 m/sec, so that the sites are of class D in the NEHRP classification. For Brownsville, $\bar{v}_s$ is 366 m/sec, which would indicate a class C soil, and although we cannot rule out that it is a class D, nearby velocities determined using surface seismic data seem to indicate a class C.

Acknowledgments

This work was funded by NEHRP grant 03HQGR0036. The conclusions presented here should not be interpreted as representing the opinion of the U.S. Geological Survey. We thank E. Woolery, M. Chapman, and an anonymous reviewer for constructive comments. E. Woolery also provided the $\bar{v}_s$ from Street *et al.* (2001) used in this study.

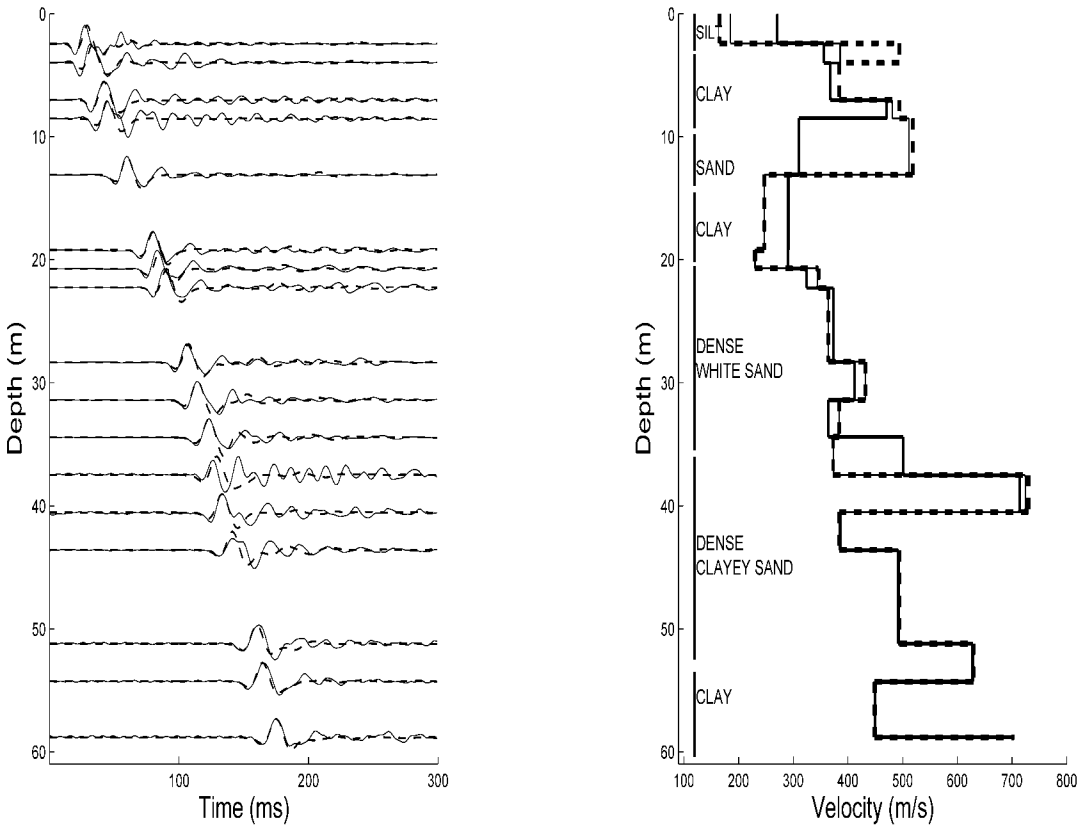

Figure 9. Similar to Figure 8 for the Jackson VSP. A Q-value of 16.4 was used. The geographic coordinates (longitude, latitude) for this site are ($-88.92°$, 35.64°).

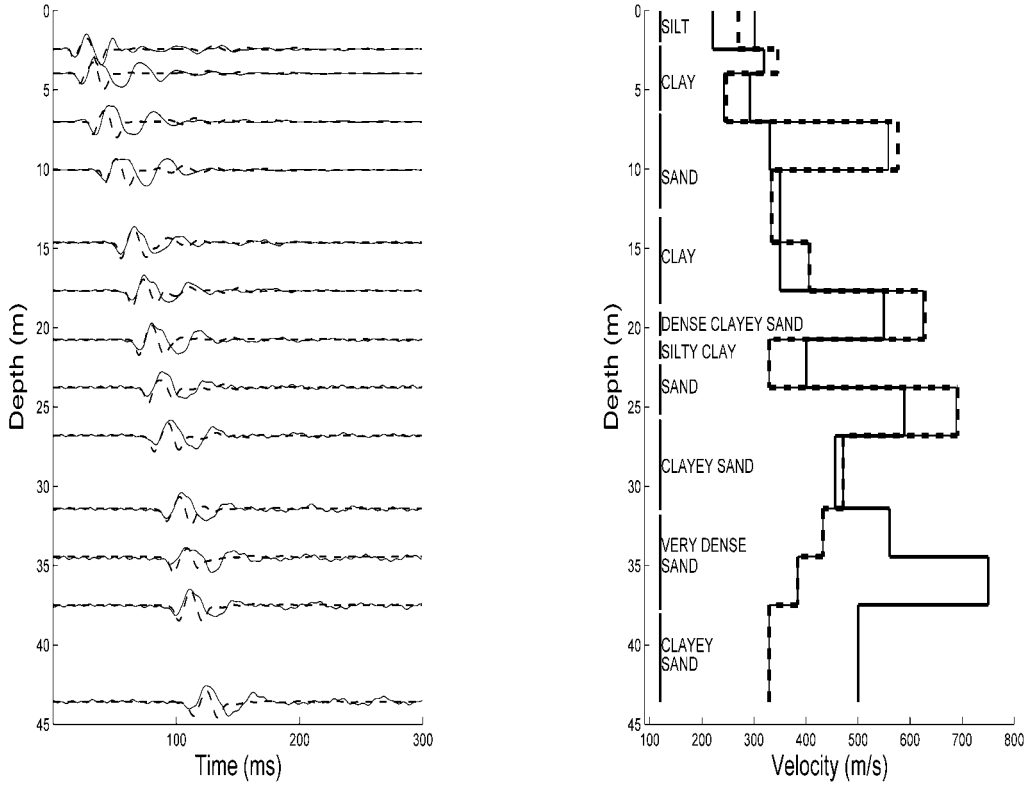

Figure 10. Similar to Figure 8 for the Brownsville VSP. A Q-value of 18.4 was used. The geographic coordinates (longitude, latitude) for this site are ($-89.26°$, 35.54°).

References

Brigham, E. (1974). *The fast Fourier Transform*, Prentice Hall, Englewood Cliffs, New Jersey.

Butler, T. (1979). Seismic attenuation studies using frequency domain synthetic seismograms, *M.Sc. Thesis*, Texas A&M University.

Chen, K. C., J. M. Chiu, and Y. T. Yang (1996). Shear-wave velocity of the sedimentary basin in the upper Mississippi embayment using *S*-to-*P* converted waves, *Bull. Seism. Soc. Am.* **86,** 848–856.

Federal Emergency Management Agency (FEMA) (1997). NEHRP recommended provisions for seismic regulations for new buildings and other structures, Part 1: Provisions (FEMA 302). Building Seismic Safety Council, Washington, D.C.

Field, E. and the SCEC Phase III Working Group (2000). Accounting for site effects in probabilistic seismic hazard analysis: overview of the SCEC Phase III report, *Bull. Seism. Soc. Am.* **90,** S1–S31.

Futterman, W. (1962). Dispersive body waves, *J. Geophys. Res.* **67,** 5279–5291.

Ge, J. (2005). Determination of shallow shear wave velocity structure and attenuation in the Mississippi embayment from VSP and refraction data, *M.Sc. Thesis*, University of Memphis.

Kane, M. F., T. G. Hildenbrand, and J. D. Hendricks (1981). Model for the tectonic evolution of the Mississippi embayment and its contemporary seismicity, *Geology* **9,** 1347–1354.

Liu, H., R. L. Maier, and R. E. Warrick (1996). An improved air-powered impulsive shear-wave source, *Bull. Seism. Soc. Am.* **86,** 530–537.

Miller, R., W. Hardeman, and D. Fullerton (1966). Geologic map of Tennessee (west sheet), Tennessee Division of Geology, scale 1:250,000.

Pujol, J. (2003). *Elastic Wave Propagation and Generation in Seismology*, Cambridge University Press, New York.

Pujol, J., R. Burridge, and S. B. Smithson (1985). Velocity determination from offset vertical seismic profiling data, *J. Geophys. Res.* **90,** 1871–1880.

Pujol, J., S. Pezeshk, Y. Zhang, and C. Zhao (2002). Unexpected values of Q_s in the unconsolidated sediments of the Mississippi embayment, *Bull. Seism. Soc. Am.* **92,** 1117–1128.

Romero, S., and G. J. Rix (2001). Regional variations in near-surface shear wave velocity in the Greater Memphis Area, *Eng. Geol.* **62,** 137–158.

Schneider, J. A., P. W. Mayne, and G. J. Rix (2001). Geotechnical site characterization in the greater Memphis area using cone penetration tests, *Eng. Geol.* **62,** 169–184.

Sherwood, J., and A. Trorey (1965). Minimum-phase and related properties of the response of a horizontally stratified absorptive earth to plane acoustic waves, *Geophysics* **30,** 191–197.

Stearns, R. G., and M. V. Marcher (1962). Late Cretaceous and subsequent structural development of the northern Mississippi Embayment area, *Geol. Soc. Am. Bull.* **73,** 1387–1394.

Stewart, R. (1983). Vertical seismic profiling: the one-dimensional forward and inverse problems, *Ph.D. Dissertation*, Massachusetts Institute of Technology.

Street, R., E. W. Woolery, Z. Wang, and J. B. Harris (2001). NEHRP soil classifications for estimating site-dependent seismic coefficients in the Upper Mississippi Embayment, *Eng. Geol.* **62,** 123–135.

Thitimarkon, T., N. Anderson, D. Hoffman, and A. Ismail (2006). A comparative analysis of 2-D MASW shear wave velocity profiling technique, *Electronic J. Geotech. Eng.* **11,** Bundle A, www.ejge.com/2006/Ppr0631/Ppr0631.htm (last accessed 18 October 2006).

Thomson, W. (1950). Transmission of elastic waves through a stratified solid medium, *J. Appl. Phys.* **21,** 89–93.

Van Arsdale, R. B., and R. K. TenBrink (2000). Late Cretaceous and Cenozoic geology of the New Madrid seismic zone, *Bull. Seism. Soc. Am.* **90,** 345–356.

Wilson, A. (1990). Computer software for the processing and interpretation of VSP data including the study of seismic wave attenuation, *M.Sc. Thesis*, Memphis State University.

Wu, R. C. (1983). Frequency domain computation of synthetic vertical seismic profiles, *M.Sc. Thesis*, Texas A & M University.

Wuenschel, P. (1960). Seismogram synthesis including multiples and transmission coefficients, *Geophysics* **25,** 106–129.

Center for Earthquake Research and Information
University of Memphis
Memphis, Tennessee 38152
(J.G.)

Department of Earth Sciences
University of Memphis
Memphis, Tennessee 38152
(J.P.)

Department of Civil Engineering
University of Memphis
Memphis, Tennessee 38152
(S.P., S.S.)

Manuscript received 16 May 2006.